Solid State Sciences 12 (2010) 1484–1489

Contents lists available at ScienceDirect

Solid State Sciences

journal homepage: www.elsevier.com/locate/ssscie

Silver(I) complexes with (1-pyrazolyl)pyridazine ligands: Synthesis, crystal structures and luminescent properties

Qun Yu, Ai-Shun Zhang, Tong-Liang Hu*, Xian-He Bu

Department of Chemistry and TKL of Metal- and Molecule-Based Material Chemistry, Nankai University, 94 Weijin Road, Tianjin 300071, PR China

ARTICLE INFO

Article history:
Received 23 January 2010
Received in revised form
2 June 2010
Accepted 10 June 2010
Available online 17 June 2010

Keywords:
Ag(I) complexes
Helical chains
Photoluminescence properties

ABSTRACT

Four Ag(I) coordination complexes formulated as $\{[Ag(\mathbf{L^1})(ClO_4)]\}_n$ (**1**), $\{[Ag(\mathbf{L^1})(NO_3)]\}_n$ (**2**), $\{[Ag(\mathbf{L^1})(PF_6)]\}_2$ (**3**) and $\{[Ag(\mathbf{L^2})](ClO_4)\cdot CH_3OH\}_n$ (**4**), ($\mathbf{L^1}$ = 3,6-bis(1-pyrazolyl)pyridazine, $\mathbf{L^2}$ = 3,6-bis(3,5-dimethyl-1-pyrazolyl)pyridazine) have been synthesized in the presence of different anions [ClO_4^- (**1**) and (**4**), NO_3^- (**2**), PF_6^- (**3**)] and structurally characterized by FT-IR spectra, elemental analysis and X-ray diffraction. Studies of X-ray diffraction reveal that complexes **1**, **2** and **4** show infinite helical chains, which are the alternate left- and right-handed helical chains. Furthermore, helical chains are arranged to 2D sheet via C–H···O (from anion O atoms) hydrogen bonds. As the anion changed to PF_6^-, a dinuclear molecule is formed in complex **3**, further constructing a 2D sheets by C–H···F hydrogen bonds. The photoluminescence properties of all the complexes **1**–**4** have been investigated in the solid state at room temperature.

1. Introduction

In the past few years, metal-organic polymeric complexes have attracted considerable interest not only for their diversity of architectures and topologies, but also for their fascinating potential application as functional materials [1]. A large number of studies have been devoted to the investigation of the diverse frameworks exhibiting multifunction, such as gas storage, separation, catalysis, photochemical activity [2]. Many factors such as the structure of the organic ligands, counterions, and weak interactions (C–H···O, C–H···F, and C–H···M close interactions and so on) have been found to remarkably influence the structure of the resultant coordination frameworks [3–7]. To understand the intriguing connection between complex structures and the influencing factors is one of the key points for the rational design of crystalline materials, but this still seems to be a long-term challenge [8].

Pyrazole, pyridazine, and their derivatives are interesting bridging ligands and are able to act as bridges between metal centers [9]. Many works have been devoted to the magnetic properties of Cu(II) and Co(II) complexes with (1-pyrazolyl)pyridazine ligands [10,11]. However, few Ag(I) complexes with this kind of ligands have been structurally characterized to date, since their scarce tendency to crystallize in common solvents and the relatively low solubility of the related ligands [12,13]. We have recently pursued the chemical reactivity of such ligands under conventional conditions. Some crystalline Ag(I) complexes with (1-pyrazolyl)pyridazine ligands have been successfully obtained.

Herein, we report the crystal structures of four new Ag(I) complexes, $\{[Ag(\mathbf{L^1})(ClO_4)]\}_n$ (**1**), $\{[Ag(\mathbf{L^1})(NO_3)]\}_n$ (**2**), $\{[Ag(\mathbf{L^1})(PF_6)]\}_2$ (**3**), and $\{[Ag(\mathbf{L^2})](ClO_4)\cdot CH_3OH\}_n$ (**4**), ($\mathbf{L^1}$ = 3,6-bis(1-pyrazolyl)pyridazine, $\mathbf{L^2}$ = 3,6-bis(3,5-dimethyl-1-pyrazolyl)pyridazine, Scheme 1), synthesized by Ag(I) ions with $\mathbf{L^1}$ and $\mathbf{L^2}$ respectively in a mixed solution of methanol and chloroform in test tube in the darkness. It is worth noting that complexes **1**, **2** and **4** comprised helical chains, which are the alternate left- and right-handed helical chains. In addition, the photoluminescence properties of complexes **1**–**4** have also been investigated in the solid state at room temperature.

2. Experimental section

2.1. Materials and general methods

The starting materials for synthesis and the solvents employed were commercially available and used as received. Ligands 3,6-bis(1-pyrazolyl)pyridazine ($\mathbf{L^1}$) 3,6-bis(3,5-dimethyl-1-pyrazolyl)pyridazine ($\mathbf{L^2}$) were synthesized according to the already published procedures [14]. IR spectra were measured on a Tensor 27 OPUS (Bruker) FT-IR spectrometer with KBr pellets. Elemental analyses (C, H and N) were performed on a Perkin–Elmer 240C analyzer. The X-ray powder diffraction (XRPD) was recorded on a Rigaku D/Max-2500 diffractometer at 40 kV, 100 mA for a Cu-target tube and

* Corresponding author. Fax: +86 22 23502458.
E-mail address: tlhu@nankai.edu.cn (T.-L. Hu).

1293-2558/$ – see front matter © 2010 Elsevier Masson SAS. All rights reserved.
doi:10.1016/j.solidstatesciences.2010.06.013

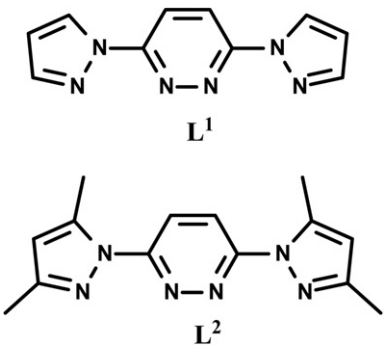

Scheme 1. The (1-pyrazolyl)pyridazine ligands $\mathbf{L^1}$ and $\mathbf{L^2}$.

a graphite monochromator. Simulation of the XRPD spectra were carried out by the single-crystal data and diffraction-crystal module of the Mercury(Hg) program available free of charge via the internet at http://www.iucr.org. Emission spectra in solid state at room temperature were taken on a Cary Eclips fluorescence spectrophotometer.

2.2. Synthesis of complexes *1–4*

$\{[Ag(\mathbf{L^1})(ClO_4)]\}_n$ (**1**). A buffer solution of methanol and chloroform (V:V = 3:1, 10 mL) was carefully layered over a chloroform solution (2 mL) of $\mathbf{L^1}$ ligand (0.1 mmol). Then, a solution of $AgClO_4$ (0.1 mmol) in methanol (2 mL) was layered over the buffer layer. Left undisturbed at room temperature and colorless single crystals was harvested after several weeks. Yield: ~45% (based on $\mathbf{L^1}$). Anal. Calcd. for $C_{10}H_8AgClN_6O_4$: C, 28.63; H, 1.92; N, 20.03. Found: C, 28.97; H, 1.58; N, 20.51. IR (KBr, cm^{-1}): 3453s, 2169w, 1635s, 1521vs, 1459vs, 1388s, 1331w, 1259 m, 1200 m, 1141 m, 1114 m, 1011s, 936vs, 890w, 852s, 761vs, 627 m, 497 m.

$\{[Ag(\mathbf{L^1})(NO_3)]\}_n$ (**2**). A procedure similar to that for **1** was followed except that $AgClO_4$ was replaced by $AgNO_3$. Yield: ~40% (based on $\mathbf{L^1}$). Anal. Calcd. for $C_{10}H_8AgN_7O_3$: C, 31.43; H, 2.11; N, 25.66. Found: C, 31.17; H, 2.35; N, 25.92. IR (KBr, cm^{-1}): 3454s, 2169w, 1635s, 1584 m, 1521s, 1457s, 1384vs, 1257w, 1199 m, 1139s, 1056 m, 1021 m, 1011s, 936s, 890 m, 851s, 761vs, 610s, 496 m.

$\{[Ag(\mathbf{L^1})(PF_6)]\}_2$ (**3**). A procedure similar to that for **1** was followed except that $AgClO_4$ was replaced by $AgPF_6$. Yield: ~40% (based on $\mathbf{L^1}$). Anal. Calcd. for $C_{20}H_{16}Ag_2F_{12}N_{12}P_2$: C, 25.83; H, 1.73; N, 18.07. Found: C, 25.79; H, 1.50; N, 18.32. IR (KBr, cm^{-1}): 3453s, 2169w, 1633s, 1585w, 1521s, 1458vs, 1388vs, 1331w, 1258 m, 1200 m, 1140s, 1056 m, 1022s, 937 m, 850vs, 761s, 610 m, 560s, 496w.

Table 2
Selected bond lengths (Å) and angles (°) for complexes **1–4**.

Complex **1**			
Ag(1)-N(6)#	2.242(3)	Ag(1)-N(1)	2.327(3)
Ag(1)-N(3)	2.366(3)	Ag(1)-N(4)	2.517(3)
N(6)#-Ag(1)-N(1)	143.85(11)	N(6)#-Ag(1)-N(3)	141.19(11)
N(1)-Ag(1)-N(3)	69.93(11)	N(6)#-Ag(1)-N(4)#	68.43(10)
N(1)-Ag(1)-N(4)#	99.03(11)	N(3)-Ag(1)-N(4)#	139.34(10)
Complex **2**			
Ag(1)-N(4)#	2.369(3)	Ag(1)-N(1)	2.265(3)
Ag(1)-N(3)	2.573(3)	Ag(1)-N(6)#	2.390(3)
N(1)-Ag(1)-N(4)#	150.39(10)	N(1)-Ag(1)-N(6)#	140.32(10)
N(4)#-Ag(1)-N(6)#	68.74(10)	N(1)-Ag(1)-N(3)	66.91(9)
N(4)#-Ag(1)-N(3)	132.63(9)	N(6)#-Ag(1)-N(3)	88.48(9)
Complex **3**			
Ag(1)-N(4)#	2.512(4)	Ag(1)-N(1)	2.435(4)
Ag(1)-N(6)#	2.244(4)	Ag(1)-N(3)	2.290(4)
N(6)#-Ag(1)-N(3)	168.49(16)	N(6)#-Ag(1)-N(1)	107.10(15)
N(3)-Ag(1)-N(1)	69.70(15)	N(6)#-Ag(1)-N(4)#	68.02(14)
N(3)-Ag(1)-N(4)#	117.06(14)	N(1)-Ag(1)-N(4)#	168.98(15)
Complex **4**			
Ag(1)-N(1)	2.147(3)	Ag(1)-N(6)#	2.148(3)
Ag(1)-N(3)	2.695(3)	Ag(1)-N(4)#	2.737(3)
N(1)-Ag(1)-N(6)#	165.19(11)	N(1)-Ag(1)-N(3)	67.96(9)
N(1)-Ag(1)-N(4)#	115.58(10)	N(3)-Ag(1)-N(4)#	145.52(9)
N(6)#-Ag(1)-N(3)	118.39(10)	N(6)#-Ag(1)-N(4)#	67.65(9)

Symmetry codes: for **1** # −x+1, y+1/2, −z+1/2; for **2** # −x+1, y+1/2, −z+1/2; for **3** # −x+2, −y+2, −z+1; for **4** # −x, y+1/2, −z+3/2.

$\{[Ag(\mathbf{L^2})](ClO_4)\cdot CH_3OH\}_n$ (**4**). A procedure similar to that for **1** was followed except that $\mathbf{L^1}$ was replaced by $\mathbf{L^2}$. Yield: ~40% (based on $\mathbf{L^2}$). Anal. Calcd. for $C_{15}H_{20}AgClN_6O_5$: C, 35.49; H, 3.97; N, 16.55. Found: C, 35.73; H, 3.67; N, 16.13. IR (KBr, cm^{-1}): 3452 m, 2024w, 1636vs, 1579 m, 1549 m, 1471w, 1427w, 1352vs, 1146 m, 1087s, 982 m, 845 m, 784w, 724 m, 624vs, 479w.

Caution! Although we met no problems in handling Ag(I) perchlorate during this work, it should be treated with great caution owing to their potential explosive nature.

2.3. X-ray data collection and structure determination

X-ray single-crystal diffraction data for complexes **1–4** were collected on a Rigaku SCX-mini diffractometer at 293(2) K. The program SAINT [15] was used for integration of the diffraction profiles. All the structures were solved by direct methods using the SHELXS program of the SHELXTL package and refined by full-matrix least-squares methods with SHELXL [16]. Ag atoms in each complex were located from the *E*-maps and other non-hydrogen atoms were located in successive difference Fourier syntheses and refined with anisotropic thermal parameters on F^2. Crystallographic data and

Table 1
Crystallographic data and structure refinement summary for complexes **1–4**.

	1	2	3	4
chemical formula	$C_{10}H_8AgClN_6O_4$	$C_{10}H_8AgN_7O_3$	$C_{20}H_{16}Ag_2F_{12}N_{12}P_2$	$C_{15}H_{20}AgClN_6O_5$
formula weight	419.53	382.08	930.09	507.68
space group	*P*21/*c*	*P*21/*c*	*P*21/*n*	*P*21/*c*
a/Å	8.8735(18)	8.8967(18)	8.4220(17)	14.438(3)
b/Å	7.0299(14)	6.7972(14)	14.361(3)	8.7782(18)
c/Å	21.691(4)	20.493(4)	12.188(2)	18.384(7)
β/°	91.71(3)	94.25(3)	100.41(3)	122.98(2)
V/Å^3	1352.5(5)	1235.8(4)	1449.9(5)	1954.5(9)
D/g cm^{-3}	2.060	2.054	2.131	1.678
Z	4	4	2	4
F(000)	824	752	904	992
μ/mm^{-1}	1.717	1.655	1.577	1.205
*R*1 [$I > 2\sigma(I)$]	0.0474	0.0411	0.0647	0.0486
*wR*2 (all data)	0.0801	0.0783	0.1214	0.1014